Knee Joint Articular Cartilage Segmentation using Radial Search Method, Visualization and Quantification

M. S. Mallikarjuna Swamy *ms_muttad@yahoo.co.in*
Department of Biomedical Engineering and Research Centre
Bapuji Institute of Engineering and Technology
Davangere-577004, Karnataka, India

Mallikarjun S. Holi *msholi@yahoo.com*
Department of Biomedical Engineering and Research Centre
Bapuji Institute of Engineering and Technology
Davangere-577004, Karnataka, India

Abstract

Knee is a complex and highly stressed joint of the human body. Articular cartilage is a smooth hyaline spongy material between the tibia and femur bones of knee joint. Cartilage morphology change is an important biomarker for the progression of osteoarthritis (OA). Magnetic Resonance Imaging (MRI) is the modality widely used to image the knee joint because of its hazard free and soft tissue contrast. Cartilage thickness measurement and visualization is useful for early detection and progression of the disease in case of OA affected patients. In the present work, knee joint MR images of normal and OA affected are processed for segmentation and visualization of cartilage using semiautomatic method. The radial search method is used with minor modifications in search area to reduce computation time. Cartilage thickness and volume is measured in lateral, medial and patellar regions of femur. The overall accuracy of measurements is determined by comparing the measurements with another semiautomatic method based on edge detection and interpolation. It is observed a good correlation between quantification of cartilage in two methods. The method takes less time for segmentation because of reduced manual steps. The reduced cartilage thickness and volume is observed in OA affected knee of different level of progression.

Keywords: Cartilage, Image Segmentation, Knee Joint, MRI, Osteoarthritis.

1. INTRODUCTION

The knee joint is the largest and most complex synovial joint of the human body. It is a major weight bearing joint of the body made up of condyles of femur, condyles of tibia and posterior surface of patella. Articular cartilage is a thin layer between the femur and tibia bones. It is a soft tissue at the end of bones that allows the joint to move freely. The knee joint contains a small amount of fluid in a cavity that lubricates the cartilage called synovial fluid. Osteoarthritis is a common disease of the knee joint affecting the elderly people. It occurs when cartilage becomes soft and gets eroded due to continuous wear and tear movements and with ageing. The OA affected knee joint often leads to inflammation, decrease in motion of joint due to stiffness, and formation of bone spurs (tiny growths of new bone). This decreases the ability of the cartilage to work as a shock absorber to reduce the impact of stress on the joints. The remaining cartilage wears down faster, and eventually, the cartilage in some regions may disappear altogether, leaving the bones to rub against one another during motion leading to formation of bone spurs. With OA, synovial fluid does not provide proper lubrication, which leads pain, inflammation and restriction of movements at the joints. There is no artificial material that can replace only the cartilage at the joint. In a clinical assessment study conducted on Indian population consisting of 362 elderly of more than 65 years, osteoarthritis was present in only 50.2% of the elderly aged 65-74 years, whereas it was 97.7% in elderly aged 84 years and above [1]. OA affected nearly 27

million Americans according to the study in 2007 [2]. After the age of 50, women are more prone OA than men [3].

1.1 MR Imaging of knee joints and clinical findings

MRI is non-invasive and repetitive imaging study of an individual is possible without side effects. The assessment of cartilage dimensions is important for the study of the progression of cartilage damage due to OA. MRI images are widely used for diagnosis of knee joint abnormalities. This imaging modality provides in-vivo and in-vitro information of anatomical structures. MRI can visualize cartilage, bone and other surrounding soft tissues distinctly. A comparison of MR evaluation of the morphology of articular cartilage with data from histology shows good correlation across those two modalities [4]. For quantification of cartilage thickness, volume and progressive assessments image processing techniques are used. Association between clinical features and MR image findings of knee joint are evaluated and it is found that a large joint effusion is associated with pain and stiffness [5]. The presence of osteophytes in the patella femoral compartment is also associated with pain. All other abnormalities in cartilage, menisci and subchondral cysts can be found in MR imaging only. The use of MRI for diagnosis and assessment of cartilage defect repairs has been studied [6]. MR imaging protocols like fat suppressed spoiled gradient echo sequence and the fast spin echo sequence are accurate and reliable for evaluating surface defects of articular cartilage. MR imaging findings in different stages of disease and correlation with clinical findings is studied [7]. Cartilage lesions, bone marrow edema pattern and meniscal lesions are well detected on MR images in patients with advanced OA. Anatomical variants in the knee are frequent findings on MRI. Thorough knowledge and familiarity with variant and its pathological nature are important for accurate interpretation of imaging studies [8].

1.2 Knee cartilage segmentation and quantification methods

Knee joint image segmentation is a very challenging task because of its complexity. Segmentation methods for knee joint can be classified into three categories based on manual intervention required, namely manual, semiautomatic and fully automatic. The manual segmentation methods are laborious and time consuming [9]. Semiautomatic methods are developed to reduce the manual intervention by automating few steps of processing. Fully automatic methods involve advanced and complex processing steps with certain limitations. Zohara et al. [10] developed a semiautomatic method, initially cartilage is segmented manually by marking the consecutive points along the articular contour curves with a typical spacing of 0.5-1.0 mm. An interpolated cubic B-spline curve is fitted for these points. Cashman et al. [9] developed an algorithm using edge detection and thresholding. Boundary discontinuities are bridged using B-spline interpolation and recursive region growing procedure is used in segmentation of bone. In radial search method developed by Poh et al. [11], a threshold method is used to detect the inner boundaries along the radial lines. The algorithm searches the boundary of cartilage from approximate center of femur bone region. In the method developed by Gamio et al. [12] Bezier splines are used. The control points are placed inside the cartilage following its shape to create a Bezier spline. Rays perpendicular to the spline on the control points are traced to find the bone cartilage interface. The edges are found based on the first derivative of brightness using bicubic interpolation along the line profiles. In the graph cut method developed by Shim et al. [13] seeds are placed manually (curvilinear marks) over specific anatomic regions. The seeds are propagated to neighboring pixels and then segmented. A fully automatic method using voxel classification is developed by Jenny et al. [14]. The algorithm is based on kNN classifier to reduce processing time. In the 2-D active contour algorithm developed by Claude et al. [15], a local coordinate system (LCS) is developed for the femoral and tibial cartilage boundaries for the measurement of thickness and volume. Tang et al. [16] proposed segmentation of articular cartilage surfaces using snakes, and a gradient vector flow (GVF) based external force. GVF snake is made more stable and converge to the correct surfaces, directional gradient is used to produce the gradient vector flow. Segmentation method is developed for multiple interacting surfaces belonging to multiple interacting objects, called LOGISMOS (layered optimal graph image segmentation of multiple objects and surfaces) by Yin et al. [17]. The approach is based on the algorithmic incorporation of multiple spatial inter relationships in a single n-dimensional graph,

and followed by graph optimization. Dodin et al. [18] segmented the cartilage by resampling the MRI in the neighborhood of the bone surface. Texture analysis techniques are optimized by filtering and then cartilage is discriminated as a bright and homogeneous tissue. This excludes soft tissues and enables the detection of the external boundary of the cartilage. A Bayesian decision criterion is used for automatic separation of the cartilage and synovial fluid. An unsupervised method is developed for segmentation and quantification of knee features by Tamez Pena et al [19].

Even though there are many algorithms developed for knee joint cartilage segmentation still there is a scope for better segmentation and precise quantification of cartilage because of the complexity involved in segmentation algorithms. In this work, a semiautomatic technique is developed to segment cartilage from knee MRI with reduced computation time and good accuracy in measurements.

2. METHODS

The knee joint MR images are obtained from JSS Medical College and Hospital, Mysore which includes normal and OA images. The MR images are obtained using Siemens 1.5T MRI system in fat suppressed spoiled gradient recalled (SPGR) image protocol. The imaging parameters for the sequence are: TR/TE: 16.3/4.7 ms, matrix: 256x256, FOV: 140 mm, slice thickness: 0.7 mm, x/y resolution: 0.365/0.365 mm. For this study approval is obtained from the hospital ethics committee to review the medical records and images of the patients who had been clinically diagnosed for knee joint problems and undergone MR imaging. The clinical sample of this study consists of 55 knee joint MRI dataset corresponding to one knee of each of 55 individuals. The study population ranged from 18 to 75 years. The MR images are processed using matlab 7.1 software for segmentation and visualization of cartilage.

The input knee MR images are preprocessed for noise removal using median filter. Median filter eliminates noise and preserves the edges in images. The cartilage is segmented using radial search method described by Poh et al. [11] with modification in search area. The processing steps for cartilage segmentation, thickness measurement, volume computations and 3D visualization are shown in Fig. 1.

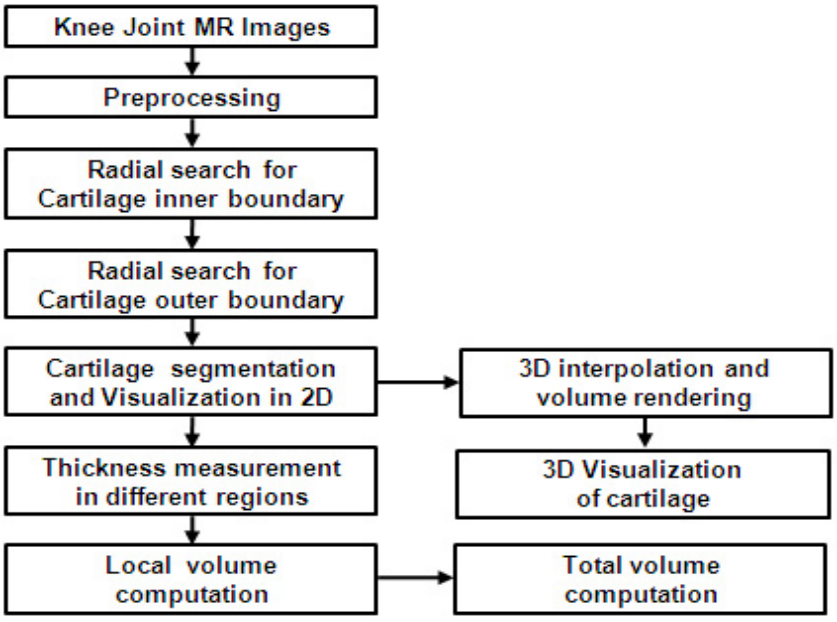

FIGURE 1: Processing steps of segmentation, thickness measurement, volume measurement and 3D visualization.

The sample points on inner boundary and outer boundary are obtained using radial search method. Using inner and outer boundary sample points a mask is developed for the cartilage. Then the cartilage is segmented from the knee MRI. The segmented cartilage thickness is computed along a normal to its inner boundary. The 2D thickness maps of cartilage in MRI sequence are saved. The voxels in between the MR slices are obtained using 3D interpolation. The articular cartilage is volume rendered using 3D texture mapping technique. The volume of the cartilage is computed by cumulatively adding the local volumes obtained.

2.1 Detection of cartilage boundary

Based on the average intensity of pixels in the cartilage region a threshold value is selected. Approximate center of the femur is selected as an origin for radii search. The search starts from this origin along a radial line. The length of the radial line is chosen to reach beyond the outer boundary. Search procedure is initiated to detect first pixel which belongs to articular cartilage along the radial line. In the inner circle of radius *r* there is no possibility of detecting the inner boundary. Therefore the search is started after *r* number of pixels away from the origin. A change in threshold level indicates the inner boundary point called b_{i1}. The coordinates of point b_{i1} are saved as inner cartilage boundary sample point. The search is continued along the next radial line which is θ° away from the previous radial line. This search results in another boundary point along the inner cartilage called b_{i2}. The search is repeated for *n* number of radial lines for an angular increment of θ° each time. The search is conducted for θ° increment from 0 to 300° which covers the different regions of cartilage. The possible boundary sample points along the inner boundary are obtained. The search is conducted for increment of 5°. This results in nearly 60 boundary sample points along the femur cartilage interface. The sample points on the boundary are further increased by interpolation. Fig. 2 depicts the radial search algorithm.

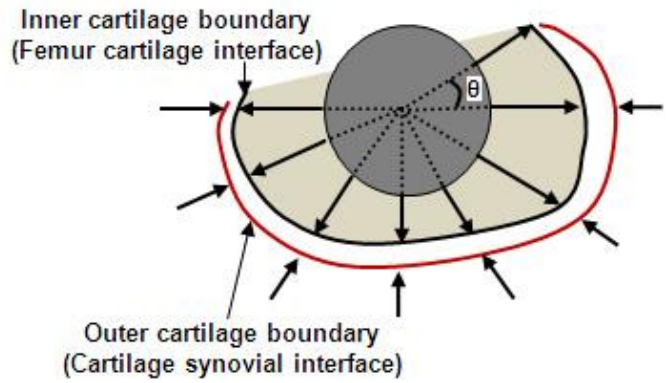

FIGURE 2: Radial search method.

Let, (x_0, y_0) is the origin of search. The search starts at r_k distance (pixels) away along the radial line from the origin. The pixel searched along a radial line is *0* to *K-1*. Search is conducted in *N* number of radial lines. The coordinate point (x_k, y_k) at which the threshold is detected is saved as boundary point. The equations of x_k and y_k are given as

$$x_k(n) = x_0 + r_k \cos(\theta_n) \tag{1}$$

$$y_k(n) = y_0 + r_k \sin(\theta_n) \tag{2}$$

where $k = 0,1.....,K-1$ and $n = 0,1,....,N$

For outer boundary detection the search is restarted along the radial line r_0 pixels away from the origin. The search is towards the origin from outside of the outer boundary. The pixel belongs to the cartilage along the radial line is searched to detect the threshold change. When the threshold level is detected, the coordinates of the pixel are saved as outer boundary point b_{o1}. The search is repeated for the radial lines drawn from 0° to 300° with an angular increment of 5°. This results in nearly 60 points along the outer boundary.

2.2 Segmentation of articular cartilage

The inner boundary sample points and outer boundary sample points of cartilage are obtained using above mentioned procedure. Fig. 3 shows the images at different steps of radial search algorithm and cartilage segmentation.

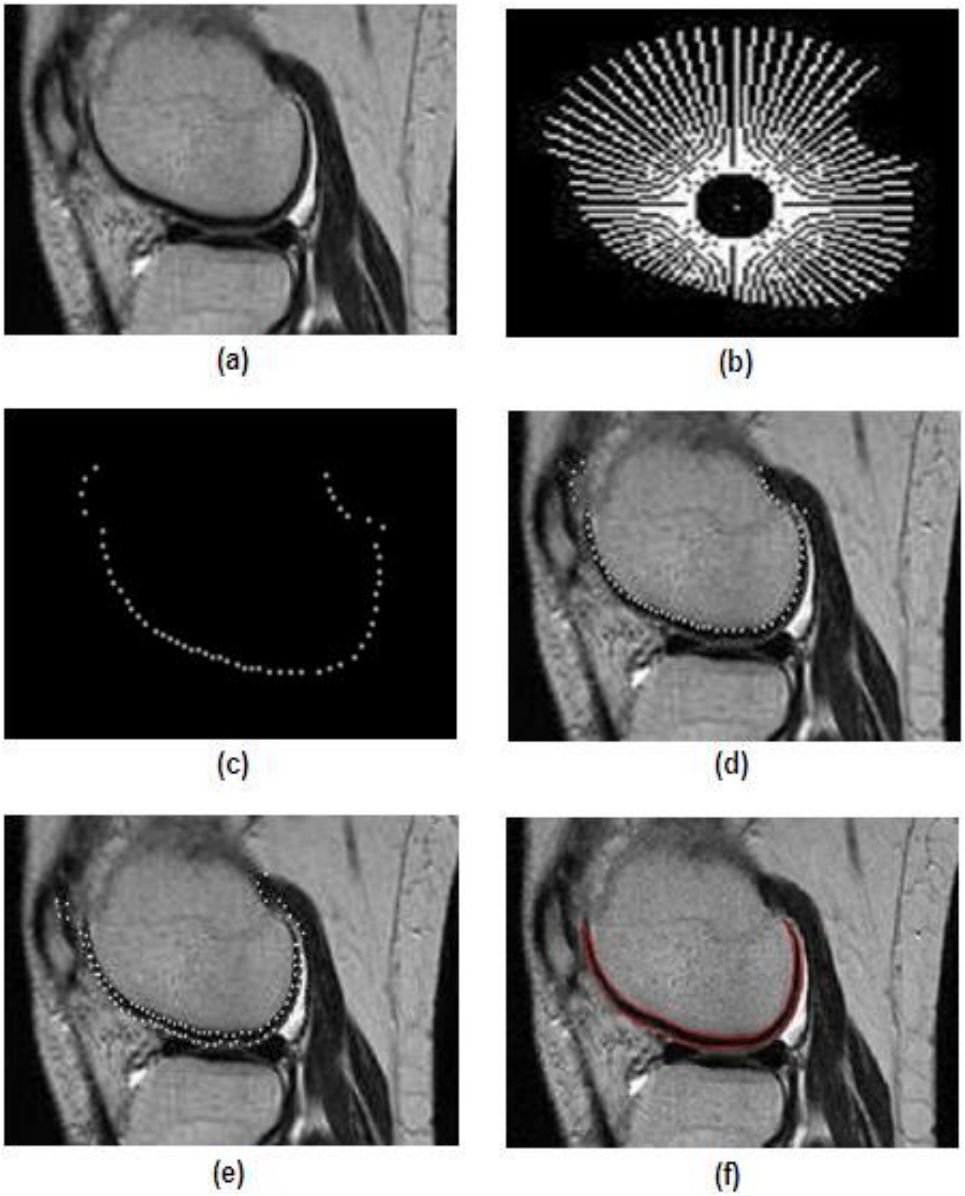

FIGURE 3: Images at different steps of processing (a) knee MR image (b) radial search (c) detection of boundary points (d) detected inner boundary points overlapped on input image (e) detected boundary points overlapped on input image (f) segmented cartilage overlapped on input image

A mask is generated using the boundary sample points. The articular cartilage is segmented from the MRI of knee joint. The manual intervention is required only to initiate the radial search process by selecting the origin of search for each image. Other processing steps are automatic.

2.3 Thickness and volume measurement of articular cartilage

The thickness of cartilage is measured in lateral, medial and patellar regions. The cartilage thickness is computed along the local normal of measurement point on the inner boundary towards the outer boundary of the cartilage. Euclidian distance between the inner boundary point b_i (x_1, y_1) to outer boundary point b_o (x_2, y_2) along the normal is computed using

$$t = \sqrt{\left(\left(x_1 - x_2 \right)^2 + \left(y_1 - y_2 \right)^2 \right)} \tag{3}$$

This results in n number of cartilage thickness (t_i) values in a region. The arithmetic mean of thickness (t_m) in a region is computed as

$$t_m = \frac{\sum t_i}{n} \tag{4}$$

The mean thickness value cartilage of a region from consecutive MRI slices is computed and average value of thickness of cartilage (t_a) in a region is calculated. The standard deviation (SD) of mean thickness from its average is computed as

$$SD = \sqrt{\frac{\sum (t_m - t_a)}{n-1}} \tag{5}$$

The coefficient of variance (COV) of cartilage thickness is computed as

$$COV = \frac{SD}{t_a} \times 100 \tag{6}$$

The local volume of cartilage is computed region wise. The total volume of cartilage in a region is summation of local volumes obtained of different regions. Volume measurement of cartilage is repeated in the same region. Average of cartilage volume (V_a) and SD is calculated. Let the total volumes in lateral, medial and patellar regions be V_l, V_m and V_p respectively. The total volume (V_T) of entire femur cartilage of knee is computed adding the volumes of different regions.

$$V_T = V_l + V_m + V_p \tag{7}$$

The segmented cartilage from MRI slice is saved as 256 x 256 size image along with its 2D texture. This is repeated for all the slices to create a stack of images of segmented cartilage. A 3D array of size (256 x 256 x 1x n) is created. The segmented cartilage images are saved into 3D array. The 3D data is volume rendered using 3D texture mapping technique. The texture is interpolated on the entire volume.

To compute the accuracy of thickness and volume of articular cartilage the measured values are compared with standard values obtained with another semiautomatic method [20] based on canny edge detection, manual marking of boundary points and B-spline interpolation. The thickness and volume of cartilage is quantified using validated semiautomatic method for the entire knee joint MRI data set. The measured thickness and volume using radial search method

are compared with the readings of the method as actual. The overall accuracy of measurements is determined using RMS (root mean square) residual difference and RMS mean error.

3. RESULTS

MR images of 55 cases including 7 normal and 48 OA affected knee joint subjects are obtained for this study. The population includes 27 male, 28 female with varying age group of 18 to 75. After computing cartilage thickness of these cases, the OA cases are separated from normal cases. The average thickness of cartilage in different regions of cartilage is measured from MRI data set of different subjects. The average cartilage thickness, SD and COV of different regions of femur of 2 normal and 4 OA affected subjects of different degree of disease severity are tabulated in Table 1.

Clinical symptom	Articular Cartilage Thickness in mm								
	Lateral			Medial			Patella		
	Avg	SD	COV	Avg	SD	COV	Avg	SD	COV
Normal1	2.08	0.06	3.54	2.04	0.05	2.75	2.15	0.13	4.86
Normal2	2.09	0.07	3.78	2.07	0.04	2.81	2.12	0.1	4.75
OA1	1.99	0.12	6.95	1.97	0.19	3.06	1.99	0.08	3.52
OA2	2.01	0.14	6.28	1.93	0.11	6.12	1.96	0.14	6.89
OA3	1.89	0.12	6.11	1.89	0.18	7.38	1.97	0.13	5.41
OA4	1.96	0.16	9.67	1.91	0.19	8.45	1.88	0.23	10.97

TABLE 1: Measured thickness of articular cartilage.

The local volumes of cartilage at different regions are computed for the MRI data set of a subject. The volume measurement of a region is repeated 3 times and average of volume measurement is computed along with SD. The Table 2 shows the computed volume of cartilage and SD in different regions for the same subjects of Table 1.

Clinical symptom	Articular cartilage volume in mm^3						Total volume ±SD
	Lateral		Medial		Patellar		
	Mean	SD	Mean	SD	Mean	SD	
Normal1	2105	118.86	2138	101.95	1173	981.6	5406
Normal2	2153	128.37	2189	107.96	1162	917.6	5491
OA1	2024	111.34	2074	116.18	1169	986.7	5282
OA2	2013	105.23	2027	129.51	1131	1038.5	5161
OA3	1996	139.68	1979	174.94	1113	1061.63	5102
OA4	1911	234.58	1925	218.03	998	1176.56	4801

TABLE 2: Measured volume of articular cartilage.

The total cartilage volume is obtained adding the volumes of cartilage of different regions. The volume is computed for normal and OA knee joints at different levels of progression. The Table 3 shows the accuracy of measurement of radial search method in comparison with measurements obtained using validated edge based method which is considered as reference. The accuracy is determined by root mean square (RMS) residual difference in measurements and RMS mean error. The measurements of cartilage at each point are compared with standard measured value and then root of the squared difference of individual measurements is computed. Percentage error of measurement is also computed in each case.

Clinical symptom	Accuracy of cartilage thickness measurement in mm								
	Lateral			Medial			Patella		
	Residual	Mean Error	Percent Error	Residual	Mean Error	Percent Error	Residual	Mean Error	Percent Error
Normal1	0.13	-0.04	1.91	0.12	-0.04	1.93	0.07	-0.02	0.93
Normal2	0.08	-0.02	0.94	0.07	-0.03	1.46	0.08	-0.01	0.47
OA1	0.09	-0.04	1.98	0.11	-0.07	3.52	0.08	0.05	2.51
OA2	0.07	-0.02	1.01	0.15	-0.08	4.06	0.12	-0.02	1.02
OA3	0.07	0.05	2.48	0.11	-0.07	3.59	0.08	0.05	2.53
OA4	0.05	-0.1	5.15	0.16	-0.12	6.22	0.11	-0.02	1.06

TABLE 3: Accuracy of cartilage thickness measurement.

Table 4 shows the overall accuracy in cartilage volume measurements with RMS residual difference and RMS mean error.

Clinical symptom	Accuracy of cartilage volume measurement in mm^3								
	Lateral			Medial			Patella		
	Residual	Mean Error	Percent Error	Residual	Mean Error	Percent Error	Residual	Mean Error	Percent Error
Normal1	12.17	-9.40	0.45	8.16	1.10	0.05	9.69	8.90	0.76
Normal2	11.31	5.20	0.24	9.42	-3.40	0.16	8.45	6.70	0.58
OA1	5.65	8.50	0.42	8.71	-1.70	0.08	5.72	2.70	0.23
OA2	7.06	-6.40	0.32	8.64	-6.10	0.30	10.47	9.90	0.88
OA3	5.28	-3.20	0.16	11.34	-6.50	0.33	9.91	-0.20	0.02
OA4	7.47	6.30	0.33	8.65	-7.70	0.40	5.99	5.10	0.52

TABLE 4: Accuracy of cartilage volume measurement.

The thickness measurements of radial search method are compared with standard measurements obtained from edge based method for all the subjects of the data set. The correlation between the cartilage thickness readings of these two methods for entire data set is in good agreement with correlation coefficient varying in the range of 0.91 to 0.97. The cartilage

thickness measurements of these two methods are plotted in Fig. 4(a) for a knee joint and computed correlation is 0.97. This indicates the good accuracy of radial search method. The deviation of cartilage thickness measurements with standard method is found less for a knee joint as indicated by the scattered plot in Fig. 4(b).

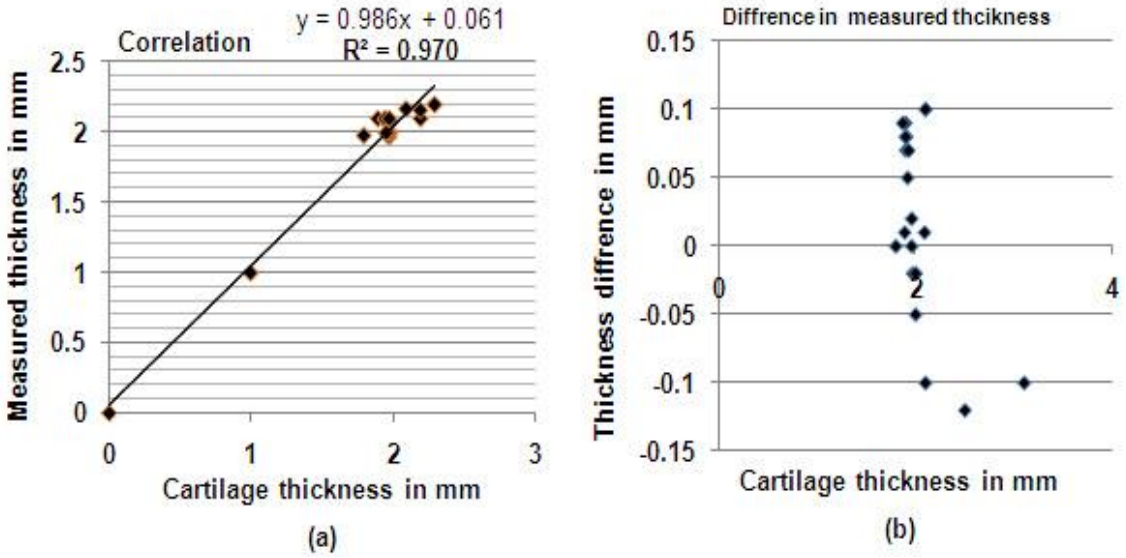

FIGURE 4: Comparison of thickness quantification results.

The thickness measured in a cartilage region for all 7 normal subjects are averaged. The cartilage thickness measured in a cartilage region for all 48 OA affected subjects are averaged. The average cartilage thickness of normal and OA affected are shown in bar chart of Fig. 5(a). The region wise cartilage volumes of normal and OA affected subjects is computed and shown in Fig. 5(b) for comparison.

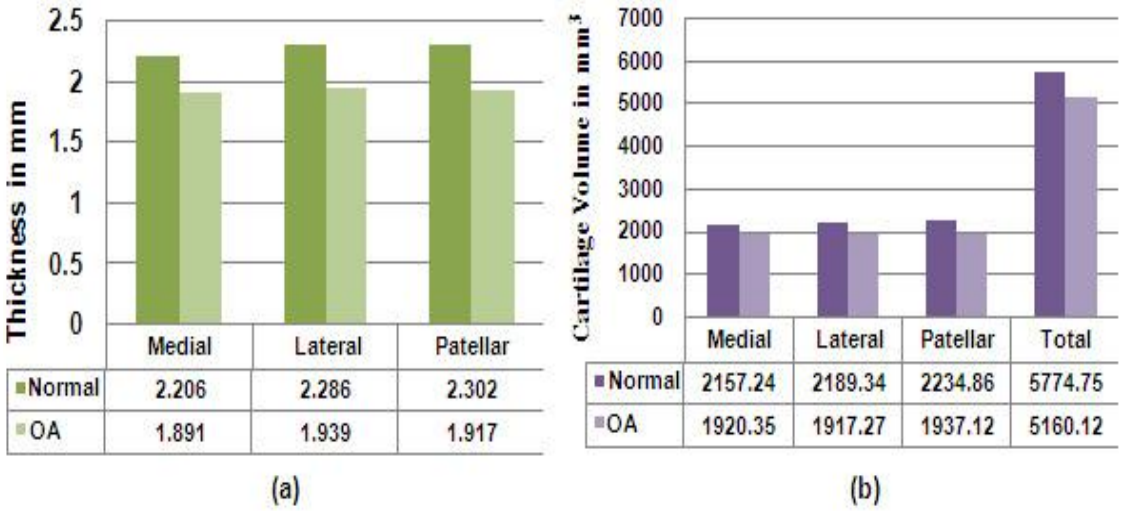

FIGURE 5: Cartilage quantification (a) average thickness (b) average volume.

The cartilage is reconstructed in 3D using texture mapping technique. The different view of visualized cartilage in 3D is shown along with its 2D visualization in Fig. 6.

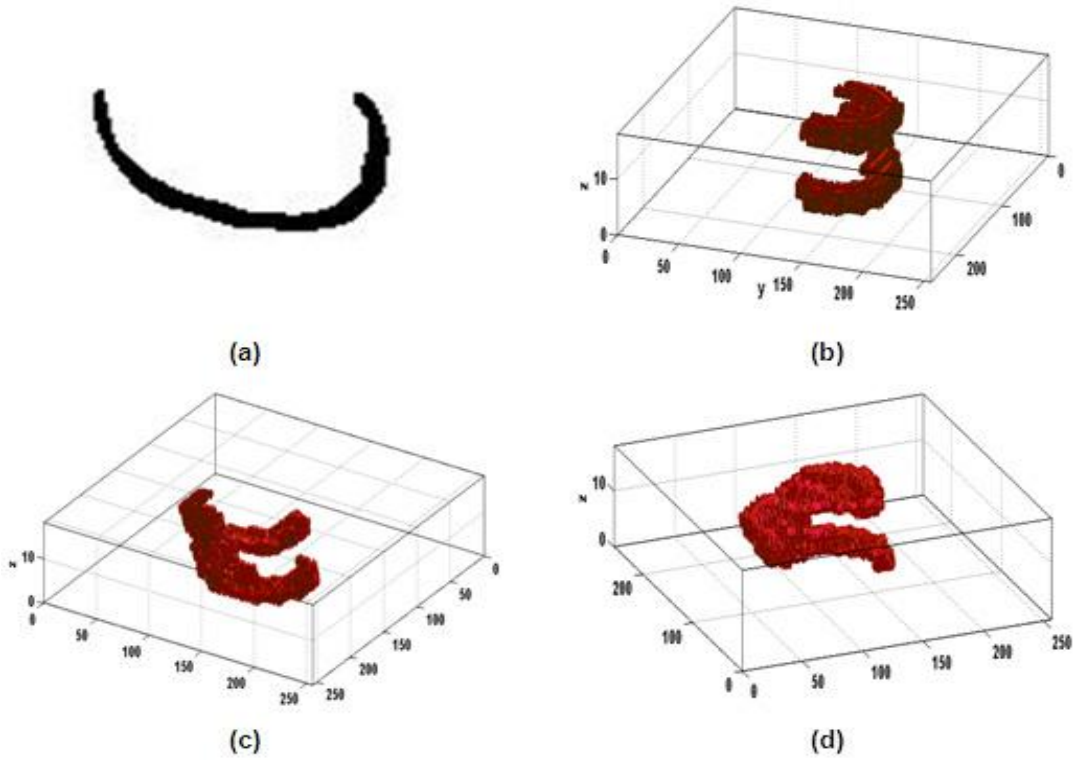

FIGURE 6: Cartilage visualization (a) cartilage in 2D (b)-(d) different views of cartilage in 3D.

4. DISCUSSION

A semiautomatic segmentation method is developed for knee cartilage segmentation from MR images of knee joint. The segmentation method is based on radial search algorithm. The method obtains the boundary points of cartilage by searching along the radial lines from marked origin. There is a modification in search procedure of radial search algorithm compared to earlier reported work [10]. In radial search algorithm the search for the cartilage interfacing boundary starts from the selected origin. In this work, the search starts *r* number of pixels away from the origin along radial line (Fig.2). The incremental angle for search lines is 5°; therefore 60 boundary points are possible for the search range of 0 to 300°. The search starts after 50 pixels along the radial line from the origin; therefore it saves more than 300 pixels to be searched for boundary points in each image of MRI sequence. During the search of outer boundary, the search starts 150 pixels away along each radial line towards the origin. This reduces the number of pixels searched for the detection of outer boundary. The number of samples on the boundary is further increased using B-spline interpolation. Selecting the origin of radial search is the only manual step in segmentation of cartilage. The total time required for processing all the images of 3D MRI sequence takes less than 5 minutes. The processing time of this method is considerably less in comparison with other semiautomatic methods.

The thickness of cartilage is measured in lateral, medial and patellar regions. The arithmetic mean of cartilage thickness is calculated in individual MR images processed. The average of cartilage thickness and SD in a region is calculated as precision measure. Out of the 55 subjects

of this study, results of few normal and OA cases are shown (Table 1). The SD is less than 0.24 in all the cases. This indicates good precision of the readings of cartilage thickness. The COV is less than 5 in normal cases and increases from 3.47 to 10.97 as the level of degradation of cartilage increases in OA cases. The COV indicates the severity of the cartilage degradation. The volume is computed in different compartments of cartilage. Initially, local volumes of cartilage are measured in consecutive images of MRI sequence region wise. To measure the repeatability of the reading, the procedure is repeated thrice on each image. The mean of the cartilage volume from these readings is calculated along with SD (Table 2). The SD is more in OA cases compared to normal cases because of the fact that thickness variations in OA are found to be abrupt. Total volume of entire femur cartilage is computed as summation of volumes in different compartments with ±SD.

The MR images of the dataset are also processed using another validated semiautomatic method of segmentation based on manual marking of boundary, edge detection, and B-spline interpolation [20]. The measurements of this method are taken as standard thickness and volume. The overall accuracy of the measurements is determined as RMS residual difference and RMS error. The RMS residual difference is less than 0.16 mm and error is less than 6.25% for cartilage thickness (Table 3). The RMS residual difference is less than 12.18mm^3 for cartilage volume and error is less than 0.89% (Table 4).

The cartilage thickness measurements obtained using radial search are compared with readings of edge detection based method as standard. The comparison shows good correlation (0.91 to 0.97) between these two methods (Fig.4a), and deviation of cartilage thickness measurements from actual value is found to be very less (Fig.4b). All the 55 subjects of data set are processed for cartilage thickness and volume measurement. The average cartilage thickness and volume of 7 normal and 48 OA cases is calculated for comparison (Fig. 5a and Fig.5b). The result indicates decreased thickness and volume in OA cases compared to normal cases. The segmented cartilage images from MRI sequence are saved and volume rendered for visualization in 3D (Fig. 6). The 3D cartilage is rotated in different directions to visualize different regions.

The modified radial search algorithm used to segment cartilage takes reduced processing time with reduced search area. The quantification of thickness and volume in normal and OA cases is carried out with precision indication. The measurements are compared with another semiautomatic method and the results are found to be in good agreement ($R^2 > 0.91$). The segmented cartilage from knee joint MRI is visualized in 2D and 3D. The reduced thickness and volumes are observed in OA affected knee joints compared to normal knee joints. The computed thickness and volume of articular cartilage is useful in the diagnosis and progressive study of OA affected patients. The results obtained agree with prior clinical diagnosis data.

The menisci (semi-lunar cartilages) at knee joint act as shock absorbers and distribute the forces of weight on the joint surfaces and provide the greater joint stability. Image processing algorithms based on MR images are useful in segmentation of menisci from knee joint. Visualization and quantification of menisci thickness, volume and detection of tears along with cartilage information is useful in diagnosis and treatment of knee abnormalities.

ACKNOWLEDGMENTS
JSS Medical College and Hospital, Mysore, Karnataka, India for providing knee MR Images

5. REFERENCES

[1] Sharma M.K., Swami H.M., Bhatia V., Verma A., Bhatia S.P.S. and Kaur G., “An epidemiological study of correlates of osteoarthritis in geriatric population of UT Chandigarh”, *Indian Journal of Community Medicine*, vol. 32, pp.77-8, 2007.

[2] Reva C.L., David T.F., Charles G.H., Lesley M.A., Hyon Choi, Richard A.D., Sherine Gabriel, Rosemarie Hirsch, Marc C.H., Gene G.H., Joanne M.J., Jeffrey N.K., Hilal Maradit K. and Frederick Wolfe, "Estimates of the prevalence of arthritis and other rheumatic conditions in the United States", *Arthritis & Rheumatism,* vol.58, pp. 26–35, 2008.

[3] Lawrence R.C., Helmick C.G., Arnett F.C., Deyo R.A., Felson David T., Giannini E.H., Heyse S.P., Hirsch R., Hochberg Marc C., Hunder G.G., Liang M.H., Pillemer S.R., Steen V.D. and Wolfe F., "Estimates of the prevalence of arthritis and selected musculoskeletal disorders in the United States", *Arthritis & Rheumatism*, vol. 41(5), pp. 778-799, 1998.

[4] Hussain Z.T. and Usha S. Sinha, "Automated image processing and analysis of cartilage MRI: enabling technology for data mining applied to osteoarthritis", *Proc. Conf. American Institute of Physics,* vol.953, 2007, pp. 262-276.

[5] Peter R.K., Johan L.B., Ruth Y.T.C., Naghmeh R., Frits R.R., Rob G.N., Wayne O.C., Marie-Pierre Hellio Le G. and Margreet K. "Osteoarthritis of the knee: association between clinical features and MR imaging findings", *Radiology,* vol.239, pp. 811-817, 2006.

[6] Stefan M., Tallal C.M., György V., Christoph R. and Siegfried T., "Magnetic resonance imaging for diagnosis and assessment of cartilage defect repairs", *Injury, Int. J. Care of the Injured, v*ol.39S1, pp.S13–S25, 2008.

[7] Thomas M.L., Lynne S.S., Srinka G., Michael R., Ying Lu, Nancy L. and Sharmila M., "Osteoarthritis: MR Imaging findings in different stages of disease and correlation with clinical findings", *Radiology*, vol. 226, pp. 373–381, 2003.

[8] Snoeckx A., Vanhoenacker F. M., Gielen J. L., Van Dyck P. and Parizel P. M., "Magnetic resonance imaging of variants of the knee", *Singapore Med Journal*, vol. 49(9), pp. 734-744, 2008.

[9] Peter M.M. Cashman., Richard I. Kitney, Munir A.G. and Mary E.C., "Automated techniques for visualization and mapping of articular cartilage in MR images of the osteoarthritic knee: a base technique for the assessment of microdamage and submicro damage", *IEEE Trans. Nanobioscience,* vol. 1, pp. 42-51, 2002.

[10] Zohara A. Cohen, Denise M.M., S. Daniel Kwak., Perrine L., Fabian F., Edward J.C., and Gerard A.A., "Knee cartilage topography, thickness, and contact areas from MRI: in-vitro calibration and in-vivo measurements", *Osteoarthritis and Cartilage,* vol.7, pp. 95–109, 1999.

[11] Poh C.L. and Richard I.K., "Viewing interfaces for segmentation and measurement results", Proc*. of 27th Annual Conf. IEEE Engineering in Medicine and Biology*, Shanghai, China, 2005, pp. 5132-5135.

[12] Julio Carballido Gamio, Jan S. Bauer, Keh-Yang Lee, Stefanie Krause and Sharmila Majumdar, "Combined image processing techniques for characterization of MRI cartilage of the knee", Proc. 27th Annual Conf. IEEE Engineering in Medicine and Biology, Shanghai, China, 2005, pp.3043-3046.

[13] Hackjoon Shim, Samuel Chang, Cheng Tao, Jin-Hong Wang, C. Kent Kwoh and Kyongtae T. Bae, "Knee cartilage: efficient and reproducible segmentation on high spatial-resolution MR images with the semi automated graph-cut algorithm method", *Radiology*, vol. 251, pp. 548-556, 2009.

[14] Jenny F., Erik B.D., Ole F.O., Paola C.P. and Claus C., "Segmenting articular cartilage automatically using a voxel classification approach", *IEEE Trans. Medical Imaging*, vol. 26, pp.106-115, 2007.

[15] Claude K., Pierre G., Benoît G., Alain G., Gilles B., Jean P.R., Johanne M.P., Jean Pierre Raynauld, Johanne M.P., Jean Pierre P. and Jacques A. de G., "Computer aided method for quantification of cartilage thickness and volume changes using MRI: validation study using a synthetic model", *IEEE Trans. Biomedical Engineering,* vol. 50, pp. 978-988, 2003.

[16] Jinshan Tang, Steven Millington, Scott T. Acton, Jeff Crandall, and Shepard Hurwitz, "Surface extraction and thickness measurement of the articular cartilage from MR images using directional gradient vector flow snakes", *IEEE Trans. Biomedical Engineering*, vol. 53, pp.896-907, 2006.

[17] Yin Yin, Xiangmin Zhang, Rachel Williams, Xiaodong Wu, Donald D. Anderson and Milan Sonka, "LOGISMOS-Layered Optimal Graph Image Segmentation of Multiple Objects and Surfaces: cartilage segmentation in the Knee Joint", *IEEE Trans. Medical Imaging*, vol. 29, pp. 2023-2037, 2010.

[18] Pierre Dodin, Jean Pierre Pelletier, Johanne Martel Pelletier and François Abram, "Automatic human knee cartilage segmentation from 3D magnetic resonance images", *IEEE Trans. Biomedical Engineering*, vol. 57, pp. 2699-2711, 2010.

[19] Jose G. Tamez Pena, Joshua Farber, Patricia C. Gonzalez, Edward Schreyer, Erika Schneider, and Saara Totterman, "Unsupervised segmentation and quantification of anatomical knee features: Data from the Osteoarthritis Initiative", *IEEE Trans. Biomedical Engineering*, vol. 59, pp.1177-1186, 2012

[20] Mallikarjunaswamy M. S. and Mallikarjun S. Holi, "Segmentation, visualization and quantification of knee joint articular cartilage using MR images", *Springer Multimedia Processing, Communication and Computing Applications*, Proc. first Int. Conf. ICMCCA, 13-15 Dec 2012, vol.213, pp.TP15/1-12.